PV Cell Orientation Angle Optimization for a Solar Energy Harvesting Base Station

Doris Benda*, Xiaoli Chu*, Sumei Sun†, Tony Q.S. Quek‡ and Alastair Buckley*
* University of Sheffield, United Kingdom
† Institute for Infocomm Research, A*STAR, Singapore
‡ Singapore University of Technology and Design, Singapore
E-mail: dcbenda1@sheffield.ac.uk, x.chu@sheffield.ac.uk, sunsm@i2r.a-star.edu.sg,
tonyquek@sutd.edu.sg, alastair.buckley@sheffield.ac.uk

***Abstract*—Photovoltaic (PV) cell powered base stations (BSs) have been widely considered for reducing the cellular network's environmental footprint in the future. An inherent challenge is to match the energy generation profile with the energy consumption profile. In this paper, we develop a Markov chain based algorithm to determine the optimal orientation angle of the PV cell for matching the two profiles, given the energy generation profile of the geo-location, the load profile of the BS and the battery capacity. We investigate the effects of different battery capacities on the optimized PV cell orientation angle for BSs located in a business district in London in summer. Our results show that the optimal orientation angle for a small battery capacity (10000 Joules at a small BS) is in the range from $35°$ to $60°$, whereas a wider range from $-50°$ to $60°$ could be chosen for a large battery capacity (50000 Joules at a small BS). This reveals that PV cell orientation angle optimization is more important for PV cell powered BSs with small battery capacities than for large battery capacities.**

***Index Terms*—Cellular network, solar powered base stations, PV cells, battery capacity, orientation angle, inclination angle**

I. Introduction

A. Related works

The accumulated energy consumption of the base stations (BSs) has become a serious burden for cellular network operators due to the rapid expansion of BSs deployment recently [1], [2], resulting in a drive to find environmental-friendly cost-effective energy sources [3]. Photovoltaic (PV) cell powered BSs have been suggested by the research community for future cellular networks [4], [5]. Whereas a main grid connected BS can always draw energy from the grid, a PV cell powered BS without grid connectivity has a characteristic energy generation profile which differs from the energy consumption profile of the BS [6]. An efficient energy generation and consumption profile matching is necessary to maximize the energy utilization of the PV cell powered BS.

Optimizing the inclination angle of PV cells to shift the energy generation profile towards the energy consumption profile of an isolated island was investigated in [7], with the objective of transferring energy from a surplus season to a shortage season on a yearly basis. The inclination angle was optimized to achieve a good match between the yearly energy generation and consumption profiles. The investigation showed that the optimal inclination angle depends on the energy consumption profile of the isolated island and differs from the inclination angle which harvests the most energy throughout the year. In cellular networks, the energy consumption of a BS changes with the data traffic load on a daily basis. Therefore, our paper will transfer the concept in [7] to the PV cell orientation angle optimization when considering the daily energy generation profile and consumption profile of a BS.

A life cycle energy cost assessment at a stand-alone PV system was conducted in [8] to evaluate the long term benefits of shifting the energy consumption profile towards the energy generation profile. A better match of both profiles led to a longer battery lifetime due to less battery charging-discharging cycles and the opportunities to downsize the battery capacity and PV cell surface area.

B. Overview - Inclination and orientation angles of PV cells

The position of a PV cell in space is uniquely defined by the orientation angle θ and the inclination angle γ. The inclination angle describes the tilt of the PV cell compared to a horizontally mounted PV cell whereas the orientation angle describes the orientation in respect to the southern direction ($\theta = 0°$). The western (eastern) direction is defined as $\theta = 90°(\theta = -90°)$ cf. Fig. 1.

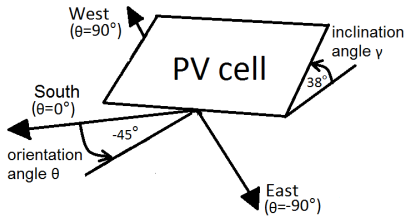

Fig. 1: Definition of the orientation angle θ and inclination angle γ of a PV cell

If the surrounding area of PV cells are free of obstructions, PV cells on the northern (southern) hemisphere should be orientated to the south $\theta = 0°$ (north $\theta = 180°$), and an inclination angle approximately equal to the latitude of the deployment site should normally be chosen to maximize the energy yield [9]. Nonetheless, an inclination angle of $10°-15°$ less than the local latitude is often practically chosen to improve the performance of the PV cell during the winter months in the temperate zone [9]. TABLE I gives an overview

978-1-5090-5019-2/17/$31.00 ©2017 IEEE

of the optimal inclination and orientation angle for PV cells located at the equator, in the northern and in the southern hemisphere.

TABLE I: Optimal orientation and inclination angle for different locations

Location	Optimal orientation angle θ	Optimal inclination angle γ
Northern hemisphere	$0°$	similar to the location's latitude
Southern hemisphere	$180°$	similar to the location's latitude
Equator	any angle between -180 and $180°$	$0°$

The more the actually installed orientation angle differs from the optimal orientation angle ($\theta = 0°$ or $\theta = 180°$), the less energy can be harvested by the PV cell during a whole day. However, the energy generation profile of the PV cell can be shifted to match the load profile of the BS, resulting in a better energy utilization. The time shift of the energy generation profile caused by changing the orientation angles is greater in the temperate zone than in areas close to the equator (cf. Fig. 2). Our previous study [10] showed that orientating PV cells to southwest ($\theta = 45°$) at BSs located in a business district in London in summer outperforms the south ($\theta = 0°$) orientated PV cells due to less wasted energy. In this paper, we extend our research and optimize the orientation angle of a solar energy harvesting BS over the wide range $\theta \in \{-50°, ..., 90°\}$. In addition, we will investigate the impact of the battery capacity on the optimal orientation angle.

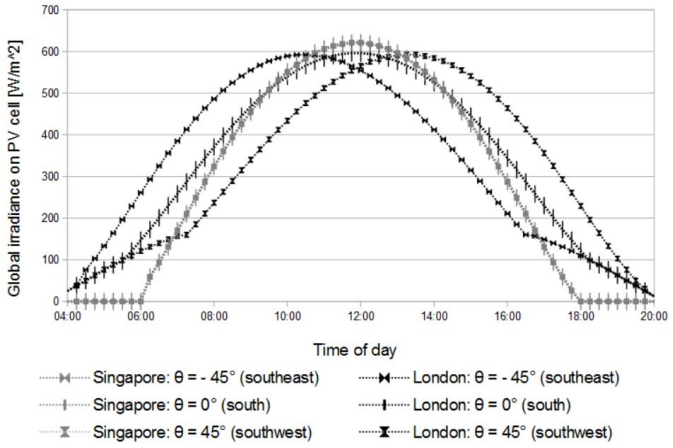

Fig. 2: Global irradiance comparison of different orientated PV cell installations in London (temperate zone in the northern hemisphere) and Singapore (close to equator) in June. An inclination angle of 38° (0°) was chosen for London (Singapore). Data source: [11]

C. Contributions and organization

We develop a Markov chain based algorithm to optimize the PV cell orientation angle of a solar powered BS, for given battery capacity, energy generation profile and energy consumption profile of the BS.

The main contributions of this paper can be summarized as follows:

- Developing a Markov chain algorithm to optimize the PV cell orientation for a PV cell powered BS so that the number of user equipment (UEs) served by the BS throughout the day $\overline{S_{\mathrm{UE}}}(\theta, \gamma)$ is maximized.
- Verifying the accuracy of the Markov chain algorithm by showing that simulation trials converge based on the law of large numbers to the output $\overline{S_{\mathrm{UE}}}(\theta, \gamma)$ of the Markov chain algorithm.
- Showing that the Markov chain algorithm (depends on the number of battery states) requires a shorter running time than the simulation trials (depends on the number of trials) for moderate battery capacities.
- Investigating the dependency of the optimal PV cell orientation angle on the given battery capacities.

The rest of this paper is organized as follows. Section II presents the system model. Section III derives the Markov chain based PV cell orientation angle optimization algorithm, which considers the PV cell orientation and inclination. Section IV-A introduces a Simulation algorithm as a baseline for the comparison and evaluation of the Markov chain algorithm. Section IV-B investigates the running time of both algorithms. Section IV-C verifies the accuracy of the Markov chain algorithm with simulation results based on a case study in a London business district in summer. Section IV-D shows the dependency of the optimal PV cell orientation angle on the battery capacities. Finally, the paper is concluded in Section V and future extension possibility for the algorithms are given.

II. System Model

The system considered in the paper is depicted in Fig. 3, which consists of a PV cell to contribute the energy generation profile, a BS to generate the energy consumption profile, and a battery to store the generated energy and supply it to the BS. The generation profile can be controlled by tuning the orientation angle of the PV cell. The objective function is to maximize the number of served UEs throughout a day.

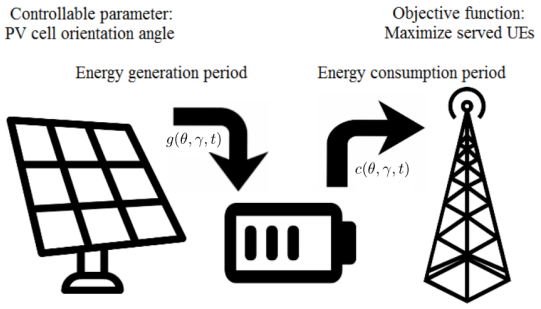

Fig. 3: System model

A. Solar energy storage model

Each BS is only powered by a PV cell. The only controllable parameter in the system model is the PV cell orientation angle, whereas all the other parameters are fixed. The day is divided into T time steps $t \in \{1, ..., T\}$. Each time step has two distinguish periods, first the energy generation period will be executed followed by the energy consumption period (cf. Fig. 3). During the energy generation period, the amount of generated energy in this time step is calculated and stored in the

battery. During the energy consumption period, the amount of consumed energy by the BS in this time step is subtracted from the battery. In reality both periods occur simultaneously. For applications that require a simultaneous energy generation and consumption, the length of the time steps can be chosen small enough to achieve a nearly simultaneous energy generation and consumption.

B. Energy generation period

The harvested solar energy $h(\theta, \gamma, t)$ at the BS in time step t is given by

$$h(\theta, \gamma, t) = G(\theta, \gamma, t) \cdot \eta \cdot A \cdot \bar{t} \tag{1}$$

where $G(\theta, \gamma, t)[W/m^2]$ is the global irradiance value in time step t on a PV cell with orientation angle θ and inclination angle γ, η is the PV cell energy conversion efficiency coefficient, $A[m^2]$ is the surface area of the PV cell, and $\bar{t}[s]$ is the length of one time step.

The time dependent global irradiance value can be obtained from the data base [11] for a given location, month, orientation and inclination angle.

The generated solar energy $g(\theta, \gamma, t)$ which is stored in the battery in time step t is given by

$$g(\theta, \gamma, t) = \min\{h(\theta, \gamma, t), b_{\max} - b_{(\theta,\gamma)}(t-1)\} \tag{2}$$

where $b_{\max}$ is the maximum battery capacity and $b_{(\theta,\gamma)}(t-1)$ is the stored energy in the battery in time step $t-1$. This equation ensures that the stored energy in the battery is less or equal the maximum battery capacity.

The stored energy is updated in time step t as follows

$$b_{(\theta,\gamma)}(t) = b_{(\theta,\gamma)}(t-1) + g(\theta, \gamma, t). \tag{3}$$

C. Energy consumption period

The consumed energy correlates with the number of UEs connected to the BS. The average number of UEs located in the coverage area of a BS follows a daily load profile (cf. Fig. 4). We use a daily load profile typical for a business district for downlink transmission. The UE density parameter $\lambda(t)$ at time step t can be calculated as follows

$$\lambda(t) = \lambda_{\%}(\lfloor t \rfloor_{\mathrm{h}}) \cdot \lambda_{\max} \tag{4}$$

where $\lambda_{\max}$ is the maximum UE density parameter in the coverage area of the BS, $\lambda_{\%}(\lfloor t \rfloor_{\mathrm{h}})$ is the user density percentage from $\lambda_{\max}$ at time step t (cf. Fig. 4 where t is rounded down to the nearest full hour)

To model the temporal fluctuation of the BS's energy consumption, the number of UEs located in the BS coverage area at time step t is modeled as a random variable $l(t)$ which follows a Poisson distribution (PD) with density parameter $\lambda(t)$.

$$l(t) := \mathrm{PD}(\lambda(t)) \tag{5}$$

The number of served UEs $s(\theta, \gamma, t)$ in time step t is given by

$$s(\theta, \gamma, t) = \min\{l(t), \lfloor b_{(\theta,\gamma)}(t)/c_{\mathrm{UE}} \rfloor\} \tag{6}$$

where $b_{(\theta,\gamma)}(t)$ is the stored energy at time step t and c_{UE} is the average amount of energy needed to serve one UE.

The consumed energy $c(\theta, \gamma, t)$ by the BS in time step t is given by

$$c(\theta, \gamma, t) = s(\theta, \gamma, t) \cdot c_{\mathrm{UE}}. \tag{7}$$

The stored energy in the battery is updated in time step t as follows

$$b_{(\theta,\gamma)}(t) = b_{(\theta,\gamma)}(t) - c(\theta, \gamma, t). \tag{8}$$

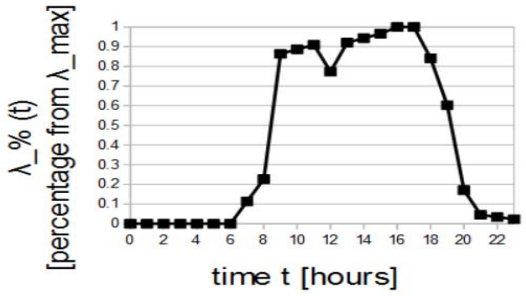

Fig. 4: Daily UE density profile of the downlink transmission in a business district. Data source: [12]

D. Determination of the average served UEs ($\overline{S_{\mathrm{UE}}}(\theta, \gamma)$)

Eq. (6) and (7) ensure that the consumed energy by the BS is less than or equal to the stored energy in the battery. As a result, it is possible that some UEs cannot be served by the BS due to a lack of energy. Therefore, we will use the number of served UEs $S_{\mathrm{UE}}(\theta, \gamma)$ throughout the day by a PV cell with orientation angle θ and inclination angle γ as the performance metric, where

$$S_{\mathrm{UE}}(\theta, \gamma) = \sum_{t=1}^{T} s(\theta, \gamma, t). \tag{9}$$

The Simulation algorithm (Algorithm 2) has to be run for a large number N until the average of the $S_{\mathrm{UE}}(\theta, \gamma)$ value converges against a fixed value denoted as $\overline{S_{\mathrm{UE}}}(\theta, \gamma)$.

The orientation angle θ which achieves the highest $\overline{S_{\mathrm{UE}}}(\theta, \gamma)$ value is considered as optimal orientation angle θ^*.

$$\theta^* = \arg\ \max_{\theta}\ \overline{S_{\mathrm{UE}}}(\theta, \gamma) \tag{10}$$

III. Markov chain algorithm

We develop the following Markov chain algorithm (Algorithm 1) to efficiently determine the optimal orientation angle of the PV cell. The advantages of the Markov chain algorithm in comparison to the Simulation algorithm (Algorithm 2) in respect to accuracy and running time will be evaluated in Section IV.

A. Markov chain initialization

We define $b_{\max} + 1$ possible battery energy states: $0, 1, 2, ..., b_{\max}$ (Joules). The expression $\mathbb{P}(b_{(\theta,\gamma)}(t) = i) = \alpha$ means that the probability of the battery having stored i Joules of energy at time step t is α.

The Markov chain algorithm (Algorithm 1 line: 4-5) uses the Eq. (1) and (4) to calculate the harvested solar energy $h(\theta, \gamma, t)$ and the UE density parameter $\lambda(t)$. The initial battery state $b_{(\theta,\gamma)}(0)$ is equal to b_{begin} at the beginning of the Markov chain algorithm. Therefore, the probability of the battery state being b_{begin} at time step 0 is 1, whereas all the other battery states have a probability of 0 (Algorithm 1 line: 8-9).

B. Energy generation period

If the PV cell harvests $h(\theta,\gamma,t)$ Joules of energy and stores the energy in the battery at time step t, then every battery state increases by $h(\theta,\gamma,t)$ Joules or reaches the maximum battery capacity $b_{\max}$ if it comes to a battery overflow. This is depicted in Fig. 5. Each transition occurs with a probability of 1, which is depicted on top of each arrow in Fig. 5. The battery states from 0 to $h(\theta,\gamma,t)-1$ have only one outgoing arrow and no incoming arrow. Therefore, the probability of the battery state being $i \in \{0,...,h(\theta,\gamma,t)-1\}$ after having stored $h(\theta,\gamma,t)$ Joules of energy is 0 (Algorithm 1 line: 13). The battery states from $h(\theta,\gamma,t)$ to $b_{\max}-1$ have exactly one incoming arrow from the battery state $h(\theta,\gamma,t)$ Joules lower. Therefore, the probability of the battery state being $i \in \{h(\theta,\gamma,t),...,b_{\max}-1\}$ is equal to the probability of the previous (at time step $t-1$) battery state $h(\theta,\gamma,t)$ Joules lower (Algorithm 1 line: 15). The battery state $b_{\max}$ has one outgoing arrow and exactly $h(\theta,\gamma,t)+1$ incoming arrows from the battery states $b_{\max}-h(\theta,\gamma,t)$ to $b_{\max}$ (Algorithm 1 line: 18).

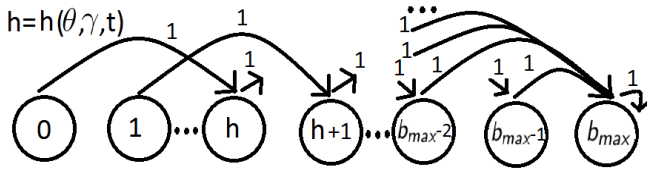

Fig. 5: Energy generation period

C. Energy consumption period

Each served UE consumes c_{UE} Joules of energy in each time step. The UEs are Poisson distributed with density parameter $\lambda(t)$. The random variable of this Poisson distribution is $l(t)=\mathrm{PD}(\lambda(t))$. The probability of $l(t)$ to be equal to an integer value r denoted as $\mathbb{P}(l(t)=r)$ is given for a Poisson distribution as $\frac{\lambda(t)^r \cdot e^{-\lambda(t)}}{r!}$ (Algorithm 1 line: 1). The expression $\mathbb{P}(l(t)\geq r)$ can also be given as $1-\sum_{w=0}^{r-1}\frac{\lambda(t)^w \cdot e^{-\lambda(t)}}{w!}$ due to the Poisson distribution of $l(t)$ (Algorithm 1 line: 2).

Next, we derive the update formulas for the battery states from c_{UE} to $b_{\max}$ (Algorithm 1 line: 31). Fig. 6 shows only the incoming arrows for the battery state c_{UE} as an example. The battery state $i \in \{c_{\mathrm{UE}},...,b_{\max}\}$ has $\lfloor (b_{\max}-i)/c_{\mathrm{UE}} \rfloor + 1$ incoming arrows. $r \in \{0,...,\lfloor (b_{\max}-i)/c_{\mathrm{UE}} \rfloor\}$ describes the transition from battery state $i+r\cdot c_{\mathrm{UE}}$ to battery state i when exactly r UEs are served. The transition probability is $\mathbb{P}(l(t)=r)$ for this transition which is depicted next to the transition arrow in Fig. 6.

The update formulas for the battery states from 0 to $c_{\mathrm{UE}}-1$ (Algorithm 1 line: 34) are derived in this paragraph. Fig. 7 shows only the incoming arrows for the battery state 0 as an example. The battery state $i \in \{0,...,c_{\mathrm{UE}}-1\}$ has $\lfloor (b_{\max}-i)/c_{\mathrm{UE}} \rfloor + 1$ incoming arrows. $r \in \{0,...,\lfloor (b_{\max}-i)/c_{\mathrm{UE}} \rfloor\}$ describes the transition from battery state $i+r\cdot c_{\mathrm{UE}}$ to battery state i when more than $r-1$ UEs are in the coverage area of the BS, which means the BS can only serve r UEs and the remaining UEs cannot be served due to the lack of available energy. The transition probability is $\mathbb{P}(l(t)\geq r)$ for this transition which is depicted next to the transition arrow in Fig. 7.

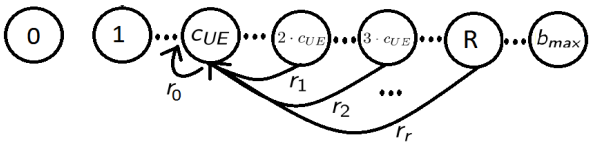

$R = \lfloor (b_{max} - c_{UE})/c_{UE} \rfloor \cdot c_{UE} + c_{UE}$
$r_0 = \mathbb{P}(\, l(t) = 0)$
$r_1 = \mathbb{P}(\, l(t) = 1)$
$r_2 = \mathbb{P}(\, l(t) = 2)$
$r_r = \mathbb{P}(\, l(t) = \lfloor (b_{max} - c_{UE})/c_{UE} \rfloor)$

Fig. 6: Energy consumption period for the battery state c_{UE}

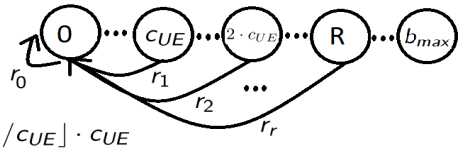

$R = \lfloor b_{max}/c_{UE} \rfloor \cdot c_{UE}$
$r_0 = \mathbb{P}(\, l(t) \geq 0)$
$r_1 = \mathbb{P}(\, l(t) \geq 1)$
$r_2 = \mathbb{P}(\, l(t) \geq 2)$
$r_r = \mathbb{P}(\, l(t) \geq \lfloor b_{max}/c_{UE} \rfloor)$

Fig. 7: Energy consumption period for the battery state 0

D. Determination of the average served UEs ($\overline{S_{\mathrm{UE}}}(\theta,\gamma)$)

When the battery is in state i, it can serve $r \in \{0,...,\lfloor i/c_{\mathrm{UE}} \rfloor\}$ UEs. When $r \in \{0,...\lfloor i/c_{\mathrm{UE}} \rfloor - 1\}$, we decrease the energy in the battery from battery state i with the transition probability of $\mathbb{P}(l(t)=r)$ and serve exactly r UEs, that is why we have to multiply the expression in Algorithm 1 line: 22 with r. When $r=\lfloor i/c_{\mathrm{UE}} \rfloor$, we decrease the energy in the battery from battery state i with the transition probability of $\mathbb{P}(l(t)\geq \lfloor i/c_{\mathrm{UE}} \rfloor)$ and serve exactly $\lfloor i/c_{\mathrm{UE}} \rfloor$ UEs, that is why we have to multiply the expression in Algorithm 1 line: 25 with $\lfloor i/c_{\mathrm{UE}} \rfloor$.

The whole Markov chain algorithm is summarized as follows

Algorithm 1 Markov chain based algorithm

Input: θ, γ, b_{begin}, $b_{\max}$, η, A, $\bar{t}$, T, $\lambda_{\max}$, c_{UE}, $G(\theta,\gamma,t)$ and $\lambda_{\%}(t) \quad \forall t$
Output: $\overline{S_{\mathrm{UE}}}(\theta,\gamma)$

1: % $\mathbb{P}(l(t)=r) = \frac{\lambda(t)^r \cdot e^{-\lambda(t)}}{r!}$
2: % $\mathbb{P}(l(t)\geq r) = 1-\sum_{w=0}^{r-1}\frac{\lambda(t)^w \cdot e^{-\lambda(t)}}{w!}$

3: **for** $t=1:T$ **do**
4: $\quad h(\theta,\gamma,t) = G(\theta,\gamma,t)\cdot\eta\cdot A\cdot\bar{t}$
5: $\quad \lambda(t) = \lambda_{\%}(\lfloor t \rfloor_{\mathrm{h}})\cdot\lambda_{\max}$
6: **end for**

7: % Initialization
8: $\mathbb{P}(b_{(\theta,\gamma)}(0)=b_{\mathrm{begin}})=1$
9: $\mathbb{P}(b_{(\theta,\gamma)}(0)=i)=0 \qquad \forall i \in \{0,...,b_{\max}\}\setminus b_{\mathrm{begin}}$
10: $\overline{S_{\mathrm{UE}}}(\theta,\gamma)=0$

for $t = 1 : T$ **do**
  % Energy generation period
  $\mathbb{P}(b_{(\theta,\gamma)}(t) = i) = 0$
    $\forall i \in \{0, ..., h(\theta, \gamma, t) - 1\}$
  $\mathbb{P}(b_{(\theta,\gamma)}(t) = i) = \mathbb{P}(b_{(\theta,\gamma)}(t-1) = i - h(\theta, \gamma, t))$
    $\forall i \in \{h(\theta, \gamma, t), ..., b_{\max} - 1\}$
  $\mathbb{P}(b_{(\theta,\gamma)}(t) = b_{\max}) =$
    $\sum_{r=b_{\max}-h(\theta,\gamma,t)}^{b_{\max}} \mathbb{P}(b_{(\theta,\gamma)}(t-1) = r)$
  % Determination of the served UEs in time step t
  for $i = 0 : b_{\max}$ **do**
    for $r = 0 : \lfloor i/c_{\mathrm{UE}} \rfloor - 1$ **do**
      $\overline{S_{\mathrm{UE}}}(\theta, \gamma) = \overline{S_{\mathrm{UE}}}(\theta, \gamma) +$
        $r \cdot \mathbb{P}(l(t) = r) \cdot \mathbb{P}(b_{(\theta,\gamma)}(t) = i)$
    end for
    $\overline{S_{\mathrm{UE}}}(\theta, \gamma) = \overline{S_{\mathrm{UE}}}(\theta, \gamma) +$
      $\lfloor i/c_{\mathrm{UE}} \rfloor \cdot \mathbb{P}(l(t) \geq \lfloor i/c_{\mathrm{UE}} \rfloor) \cdot \mathbb{P}(b_{(\theta,\gamma)}(t) = i)$
  end for
  % Energy consumption period
  $\mathbb{P}(b_{(\theta,\gamma)}(t-1) = i) = \mathbb{P}(b_{(\theta,\gamma)}(t) = i)$
    $\forall i \in \{0, ..., b_{\max}\}$
  $\mathbb{P}(b_{(\theta,\gamma)}(t) = i) = \sum_{r=0}^{\lfloor (b_{\max}-i)/c_{\mathrm{UE}} \rfloor} \mathbb{P}(l(t) = r) \cdot$
    $\mathbb{P}(b_{(\theta,\gamma)}(t-1) = i + r \cdot c_{\mathrm{UE}})$
    $\forall i \in \{c_{\mathrm{UE}}, ..., b_{\max}\}$
  $\mathbb{P}(b_{(\theta,\gamma)}(t) = i) = \sum_{r=0}^{\lfloor (b_{\max}-i)/c_{\mathrm{UE}} \rfloor} \mathbb{P}(l(t) \geq r) \cdot$
    $\mathbb{P}(b_{(\theta,\gamma)}(t-1) = i + r \cdot c_{\mathrm{UE}})$
    $\forall i \in \{0, ..., c_{\mathrm{UE}} - 1\}$
end for
return $\overline{S_{\mathrm{UE}}}(\theta, \gamma)$

IV. Results and Discussion

A. Simulation algorithm

We use Eq. (1)-(10) to derive the below Simulation algorithm (Algorithm 2). Algorithm 2 is the baseline for the performance comparison with the previous shown Markov chain algorithm (Algorithm 1).

Algorithm 2 Simulation algorithm

Input: θ, γ, N, b_{begin}, $b_{\max}$, η, A, $\bar{t}$, T, $\lambda_{\max}$, c_{UE}, $G(\theta, \gamma, t)$ and $\lambda_{\%}(t)$ $\forall t$
Output: $\overline{S_{\mathrm{UE}}}(\theta, \gamma)$
$\overline{S_{\mathrm{UE}}}(\theta, \gamma) = 0$
for $n = 1 : N$ **do**
  $b_{(\theta,\gamma)}(0) = b_{\mathrm{begin}}$ % Initialization
  for $t = 1 : T$ **do**
    % Energy generation period
    $b_{(\theta,\gamma)}(t) = b_{(\theta,\gamma)}(t-1)$
      $+ \min\{G(\theta, \gamma, t) \cdot \eta \cdot A \cdot \bar{t}, b_{\max} - b_{(\theta,\gamma)}(t-1)\}$
    % Energy consumption period
    $\lambda(t) = \lambda_{\%}(\lfloor t \rfloor_{\mathrm{h}}) \cdot \lambda_{\max}$
    $s(\theta, \gamma, t) = \min\{\mathrm{PD}(\lambda(t)), \lfloor b_{(\theta,\gamma)}(t)/c_{\mathrm{UE}} \rfloor\}$
    $b_{(\theta,\gamma)}(t) = b_{(\theta,\gamma)}(t) - s(\theta, \gamma, t) \cdot c_{\mathrm{UE}}$
  end for
  $\overline{S_{\mathrm{UE}}}(\theta, \gamma) = \overline{S_{\mathrm{UE}}}(\theta, \gamma) + \sum_{t=1}^{T} s(\theta, \gamma, t)$
end for
return $\overline{S_{\mathrm{UE}}}(\theta, \gamma)/N$

B. Running Time

The Simulation algorithm has a running time of $\mathcal{O}(N \cdot T)$ whereas the Markov chain algorithm has a running time of $\mathcal{O}(b_{\max}^2 \cdot T)$. Therefore the Markov chain algorithm outperforms the Simulation algorithm when the battery is not divided into too many battery states $b_{\max}$. Especially for small BSs with small battery capacities, the Markov chain algorithm is an effective tool to determine the optimal PV cell orientation. Nonetheless choosing a lower battery resolution for larger batteries (defining a small range of Joule values as one battery state instead of using a separate battery state for each Joule value as we did in our system model) will help to reduce the computational complexity.

C. Accuracy

We use the parameters in TABLE II for the Simulation algorithm and Markov chain algorithm. Both algorithms were run for every orientation angle $\theta \in \{-50°, -45°, ..., 85°, 90°\}$ with constant inclination angle $\gamma = 38°$ (optimal inclination angle for London). The Simulation algorithm was run $N = 100000$ times to achieve a good convergence.

TABLE II: Parameters for the Simulation algorithm and Markov chain algorithm

Parameter	Value
Month	June
London	51°30′26″ North, 0°7′39″ West
θ and γ	$\theta \in \{-50°, -45°, ..., 85°, 90°\}$ and $\gamma = 38°$
N	100000
b_{begin} and $b_{\max}$	$b_{\mathrm{begin}} = 0$ J and $b_{\max} = 10000$ J
η	0.15
A	0.02 m^2
T and $\bar{t}$	$T = 96$ and $\bar{t} = 15 \cdot 60$ s
$\lambda_{\max}$	1.5 UEs per BS coverage area
c_{UE}	1500 J
$G(\theta, \gamma, t)$ and $\lambda_{\%}(t)$	cf. database [11] and Fig. 4

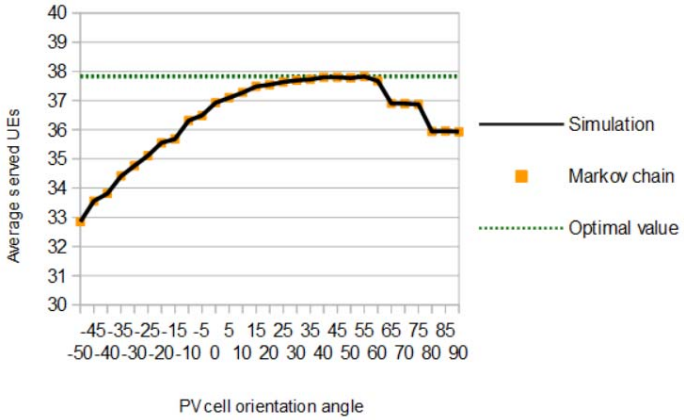

Fig. 8: PV cell orientation angle θ vs. average served UEs $\overline{S_{\mathrm{UE}}}(\theta, 38°)$

Fig. 8 compares the Simulation algorithm and the Markov chain algorithm. It shows that the Simulation algorithm and the Markov chain algorithm calculate the same $\overline{S_{\mathrm{UE}}}(\theta, 38°)$ value for each orientation angle θ ($N = 100000$). Therefore our proposed Markov chain algorithm accurate describes the limit of the Simulation algorithm convergence.

D. Dependency of the optimal PV cell orientation angle on the given battery capacities

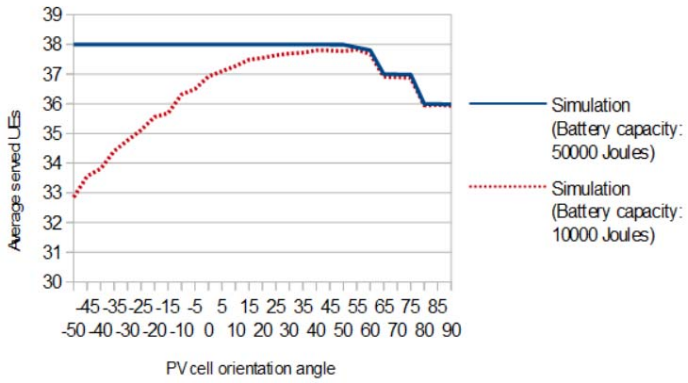

Fig. 9: PV cell orientation angle θ vs. average served UEs $\overline{S_{\mathrm{UE}}}(\theta, 38°)$ for different battery capacities

Fig. 9 plots the PV cell orientation angle θ versus the average served UEs $\overline{S_{\mathrm{UE}}}(\theta, 38°)$ for the two battery capacities 10000 Joules and 50000 Joules. Fig. 9 shows that not only the given energy generation and consumption profile is important for the outcome of the optimization but also the battery capacity. If the battery capacity is small (e.g. 10000 Joules), a lot of energy is wasted in the morning and midday hours whereas UEs cannot be served in the afternoon due to a lack of available stored energy in the battery. Therefore PV cells orientated to the west between $35°$ to $60°$ outperform the other orientation angles because the west orientated PV cells shift the energy generation towards the load profile. Figs. 8 and 9 show a significant different behavior for orientation angles above $60°$, this is mainly caused by the great misalignment, which results in a significant drop in the total energy generation of the PV cell throughout the day. This loss of the total energy generation cannot be compensated anymore by the shifted energy generation towards the consumption profile.

If the battery capacity is large (e.g. 50000 Joules), less energy is wasted in the morning and midday hours due to the larger battery capacity. All PV cell orientations can store energy generated in the morning and during midday and serve the UEs with this stored energy in the afternoon. Therefore every orientation angle between $-50°$ and $60°$ can be chosen as optimal orientation angle.

V. Conclusions and Future Extension

We have developed an algorithm to optimize the PV cell orientation of a PV cell powered BS with battery given its energy generation profile, load profile and battery capacity. The algorithm is based on a Markov chain and has a running time dependent on the squared battery resolution and time resolution. The importance of the PV cell orientation optimization was verified for a BS with small battery capacity located in a business district in London in summer. Also PV cells are normally orientated to the south in London, our algorithm revealed that the optimal orientation angle is between $35°$ to $60°$ to the west. This is caused by the ability to shift the energy generation profile towards the load profile when orientating PV cells to the west. Whereas BSs with small battery capacities significantly improved their performance by choosing the optimal orientation angle, BSs with large battery capacities have similar performance for all orientation angles between $-50°$ to $60°$ due to their ability to store energy during a surplus period and provide it during a shortage period.

Our algorithm can equivalently be used to optimize the inclination angle to achieve a better match between the yearly energy generation and consumption profiles or to optimize both angles simultaneously for a better yearly and daily match of the profiles. Also we used a business district in London in summer as case study area, the algorithm can be used for any load profile, geo-location, time of the year and battery capacity.

References

[1] G. Piro, M. Miozzo, G. Forte, N. Baldo, L. A. Grieco, G. Boggia, and P. Dini, "Hetnets powered by renewable energy sources: Sustainable next-generation cellular networks," *IEEE Internet Computing*, vol. 17, no. 1, pp. 32–39, Jan 2013.

[2] H. Zhang, X. Chu, W. Guo, and S. Wang, "Coexistence of wi-fi and heterogeneous small cell networks sharing unlicensed spectrum," *IEEE Communications Magazine*, vol. 53, no. 3, pp. 158–164, March 2015.

[3] H. Wang, H. Li, C. Tang, L. Ye, X. Chen, H. Tang, and S. Ci, "Modeling, metrics, and optimal design for solar energy-powered base station system," *EURASIP Journal on Wireless Communications and Networking*, vol. 2015, no. 1, p. 39, 2015.

[4] Y. Mao, Y. Luo, J. Zhang, and K. B. Letaief, "Energy harvesting small cell networks: feasibility, deployment, and operation," *IEEE Communications Magazine*, vol. 53, no. 6, pp. 94–101, June 2015.

[5] A. Kwasinski and A. Kwasinski, "Increasing sustainability and resiliency of cellular network infrastructure by harvesting renewable energy," *IEEE Communications Magazine*, vol. 53, no. 4, pp. 110–116, April 2015.

[6] T. Han and N. Ansari, "Powering mobile networks with green energy," *IEEE Wireless Communications*, vol. 21, no. 1, pp. 90–96, February 2014.

[7] A. H. Khan, K. R. Zafreen, A. Islam, and M. Islam, "Shifting generation of energy of solar pv using optang method-case study sandwip area," in *2015 3rd International Conference on Green Energy and Technology (ICGET)*, Sept 2015, pp. 1–5.

[8] Y. Thiaux, J. Seigneurbieux, B. Multon, and H. B. Ahmed, "Load profile impact on the gross energy requirement of stand-alone photovoltaic systems," *Renewable Energy*, vol. 35, no. 3, pp. 602 – 613, 2010.

[9] A. Luque and S. Hegedus, *Handbook of Photovoltaic Science and Engineering*, 2nd ed. John Wiley & Sons, 2011.

[10] D. Benda, X. Chu, S. Sun, T. Q. Quek, and A. Buckley, "Pv cell angle optimisation for energy arrival-consumption matching in a solar energy harvesting cellular network," *IEEE International Conference on Communications*, May 2017.

[11] European Commission. (2016) Photovoltaic geographical information system (pvgis). [Online]. Available: http://re.jrc.ec.europa.eu/pvgis/

[12] CelPlan. (2014) White paper - customer experience optimization in wireless networks. [Online]. Available: http://www.celplan.com/resources/whitepapers/Customer%20Experience%20Optimization%20rev3.pdf